THE JOURNAL OF PHYSICAL CHEMISTRY Letters

Letter

Cite This: J. Phys. Chem. Lett. 2017, 8, 5222-5227

pubs.acs.org/JPCL

Impact of Electronic State Mixing on the Photoisomerization Time Scale of the Retinal Chromophore

Madushanka Manathunga,[†] Xuchun Yang,[†] Yoelvis Orozco-Gonzalez,[†,§] and Massimo Olivucci*[,†,‡,§]

[†]Department of Chemistry, Bowling Green State University, Bowling Green, Ohio 43403, United States

[‡]Dipartimento di Biotecnologie, Chimica e Farmacia, Università di Siena, via A. Moro 2, I-53100 Siena, Italy

[§]Institut de Physique et Chimie des Matériaux de Strasbourg, UMR 7504 Université de Strasbourg-CNRS, F-67034 Strasbourg, France

Supporting Information

ABSTRACT: Spectral data show that the photoisomerization of retinal protonated Schiff base (rPSB) chromophores occurs on a 100 fs time scale or less in vertebrate rhodopsins, it is several times slower in microbial rhodopsins and it is between one and 2 orders of magnitude slower in solution. These time scale variations have been attributed to specific modifications of the topography of the first excited state potential energy surface of the chromophore. However, it is presently not clear which specific environment effects (e.g., electrostatic, electronic, or steric) are responsible for changing the surface topography. Here, we use QM/MM models and excited state trajectory computations to provide evidence for an increase in electronic mixing between the first and the second excited state of the chromophore when going from vertebrate rhodopsin to the solution environments. Ultimately, we argue that a correlation between the lifetime of the first excited state and electronic mixing between such state and its higher neighbor, may have been exploited to evolve rhodopsins toward faster isomerization and, possibly, light-sensitivity.

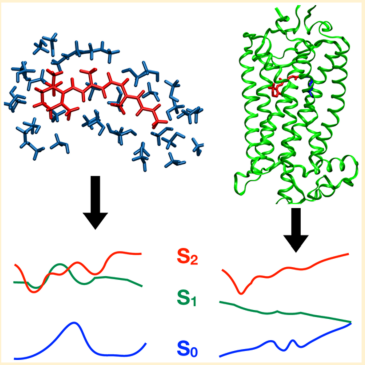

Rhodopsins are a vast family of membrane proteins found in all life domains.[1−3] In spite of their marked sequence diversity (e.g., between microbial and animal members), rhodopsins share a common architecture[1] characterized by a protonated Schiff base of retinal (rPSB) hosted in a cavity formed by seven interconnected transmembrane alpha helices. In the presence of light of suitable wavelengths, rPSB is electronically excited and undergoes a double bond isomerization which initiates various functions such as vision in vertebrates and invertebrates and ion-pumping or ion channeling in microrganisms.[3] Remarkably, such isomerization occurs on a femtosecond to picosecond time scale.[2,3] For instance, in bovine rhodopsin (Rh), the 11-*cis* rPSB chromophore (rPSB11) abandons the electronically excited state within 100 fs[4] producing a detectable photoproduct in 200 fs[5,6] while in the dark-adapted form of a sensory rhodopsin found in the cyanobacterium Anabaena PCC7120 (ASR_{AT}), an all-*trans* rPSB chromophore (rPSBAT) decays in less than 1 ps (500−700 fs) and isomerizes within 4 ps.[7−9] These fast times become significantly longer when rPSB is eletronically excited in solution (e.g., in methanol), where canonical spectroscopic studies,[10−14] shows an excited state decay within 4 ps and photoproduct formation in 15 ps.

The above observations indicate that changes in the chromophore environment (e.g., protein vs solution) must modify the shape of the potential energy surface (PES) driving the excited state dynamics.[11,14,15] However, according to a recent study,[12] rPSB11 in methanol solution would decay via two independent processes with 4 ps and 100 fs time scales. The authors hypothesize that these processes are associated with the decay of the 12-s-*cis* and 12-s-*trans* conformer of rPSB11, respectively. Since the 12-s-*trans* conformers is the one present in Rh, the authors propose that the observed 100 fs decay of such photoreceptor is an intrinsic property of its chromophore which would not be modified by the solution or protein environment.

It is apparent that, understanding the factors governing the isomerization time scale in different environments, is not only of fundamental importance for explaining the diversity of rhodopsins or probing the rPSB11 mechanism mentioned above, but also for aiding the design of biomimetic molecular devices.[16,17] Below we provide computational evidence that one factor, the electronic mixing between the first two singlet excited states (S_1 and S_2) of the rPSB chromophore, is modulated by the chromophore environment and has a strong impact on the isomerization time scale. To do so, we investigate the excited state reactivity of rPSB in methanol and two protein environments. This is done by employing an established quantum mechanics/molecular mechanics (QM/MM) approach combined with Franck−Condon (FC) trajectory computations (see the SI for details). More specifically, we use QM/MM models to comparatively study the dynamics of rPSBs along short (i.e., 100 fs) trajectories released with zero initial velocities along the S_1 PES. Consistently with previous

Received: September 2, 2017
Accepted: October 5, 2017
Published: October 5, 2017

DOI: 10.1021/acs.jpclett.7b02344
J. Phys. Chem. Lett. 2017, 8, 5222−5227

Scheme 1. Characterization of a Simplified Gas-Phase rPSB Model (PSB5) of rPSBAT[a]

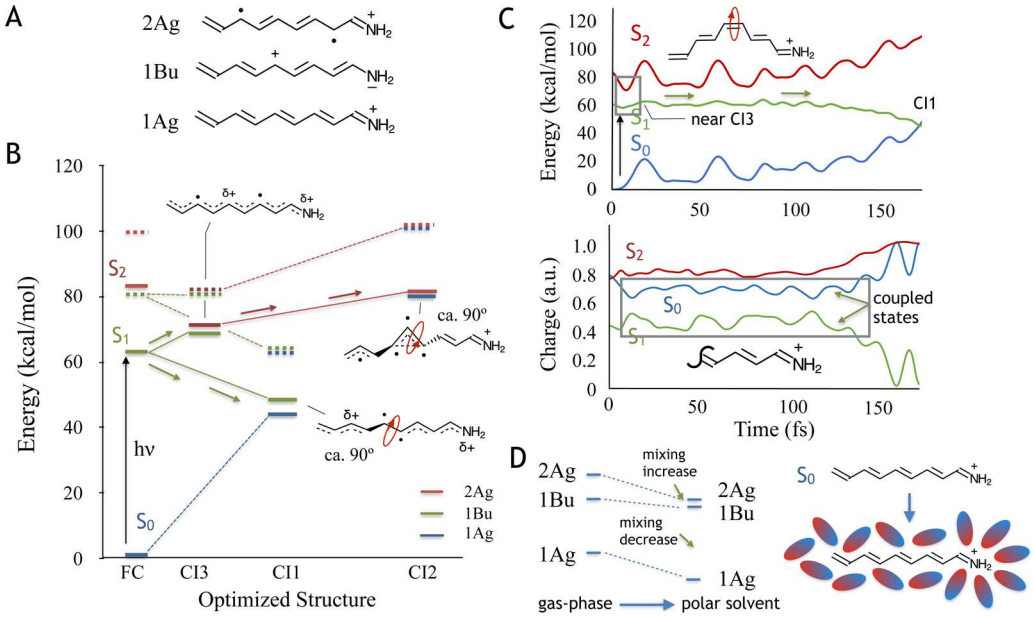

[a](A) Resonance formulas representing the dominating electronic structures of the S_0 (bottom), S_1 (middle) and S_2 (top) states of PSB5 at the FC point. (B) Relative CASPT2 (full lines) and CASSCF (dotted lines) energies of the S_0, S_1 and S_2 PESs at the FC point and 1Bu/1Ag (CI1), 2Ag/1Ag (CI2), and 2Ag/1Bu (CI3) CIs. The formulas show the "hybrid" charge distribution and unpaired electrons at each CI. The curly arrows indicate isomerizing double bonds. Along the abscissa the CIs including the spectroscopic state (i.e., CI3 and CI1) are represented geometrically closer to FC, and among these, CI3 is considered the closest since S_2 is the energetically closer to S_1. (C) Top panel: 3-root-state-average CASPT2//CASSCF/AMBER energy profiles along the FC trajectory of a 11-*cis* PSB5 model released with a 10 degrees pre-twisted central double bond (see curly arrows). Bottom panel: Evolution of the positive charge of the displayed moiety along the same trajectory. (D) Schematic representation of the effect of a polar solvent on PESs of states dominated by 2Ag, 1Bu and 1Ag characters.

studies,[4,18,19] we assume that, on such a short time scale, "FC trajectories" provide information on the dynamics of the entire populations of the system (i.e., of the center of the vibrational wave packet).

In our QM/MM approach, the geometrical progression along the trajectories is computed using 3-root-state-average CASSCF/AMBER gradients[19] and then, in order to account for the effect of dynamic electron correlation, the trajectory S_0, S_1, and S_2 energy profiles are recomputed using the CASPT2 level of theory[20] as well as the XMCQDPT2 level of theory[21] (as mentioned in the SI, XMCQDPT2 allows for a more correct description of the PESs of the mixing states (i.e., roots) included in the averaging). Notice that the energy profiles and charge distribution are not invariant with respect to the state averaging level. For this reason, FC trajectories recomputed at the 4- and 5-root-state-average CASSCF levels, are used to study the properties of our reference 3-root-state-average models.

In order to interpret the results, we now revise the main features of the low-lying PESs of gas-phase rPSBs using a simplified model featuring five double bonds (PSB5). As shown in Scheme 1A and 1B, the electronic structures (characters) contributing to the 3-root-state-average CASSCF wave functions of PSB5 are labeled 1Ag, 1Bu, and 2Ag. At the FC point (i.e., at the S_0 equilibrium structure) the S_1 PES has a 1Bu charge-transfer (CT) character. In fact, such a CT character implies that the positive charge is located near the $H_2C{=}CH-$ end of the PSB5 framework, and that its charge distribution is different from that of S_0 which has 1Ag covalent character with a positive charge located on the $C{=}NH_2$ framework end. By contrast, the S_2 PES has 2Ag diradical (DIR) character and features, similar to 1Ag, a positive charge located on the $C{=}NH_2$ group.

The PSB5 calculations yield three important results. First, as shown in Scheme 1B, the CASPT2 topology is similar to the CASSCF topology (although, as expected, the CASPT2 energy is red-shifted due to the inclusion of dynamic electron correlation). Second, three different conical intersections (CI1, CI2, and CI3) may be reached from the FC point (see Figure S3 for detailed geometries of these CIs). CI1 corresponds to a crossing between PESs with 1Ag and 1Bu characters, CI2 corresponds to a crossing between PESs with 1Ag and the 2Ag characters while CI3 is an intersection between PESs with 1Bu and 2Ag characters. Third, one can use the charge computed along a suitable chromophore moiety, to learn about the interaction between the different PESs and their electronic characters. In fact, consistently with the formulas of Scheme 1A, the $-CH-CH{=}CH-CH{=}NH2$ moiety of Scheme 1C would have a large positive charge in a 1Ag and 2Ag state but a small charge in a 1Bu state. Using such assignments, one can observe that, along the FC trajectory of Scheme 1C, the S_1 PES displays an oscillating 1Bu character (see bottom panel). Such oscillations are in a clear out-of-phase relationship with oscillations occurring along the S_0 PES associated with a dominating 1Ag character (see framed region in the bottom panel). The S_1 and S_0 PESs must thus be interacting electronically as they partially exchange their characters. Notice that here the rPSB charge distribution is evaluated at the CASSCF level for consistency with the geometrical progression. Scheme 1C also shows that such mixing continues until decay at a S_1/S_0 conical intersection (CI1) in ca. 150 fs.

DOI: 10.1021/acs.jpclett.7b02344
J. Phys. Chem. Lett. 2017, 8, 5222−5227

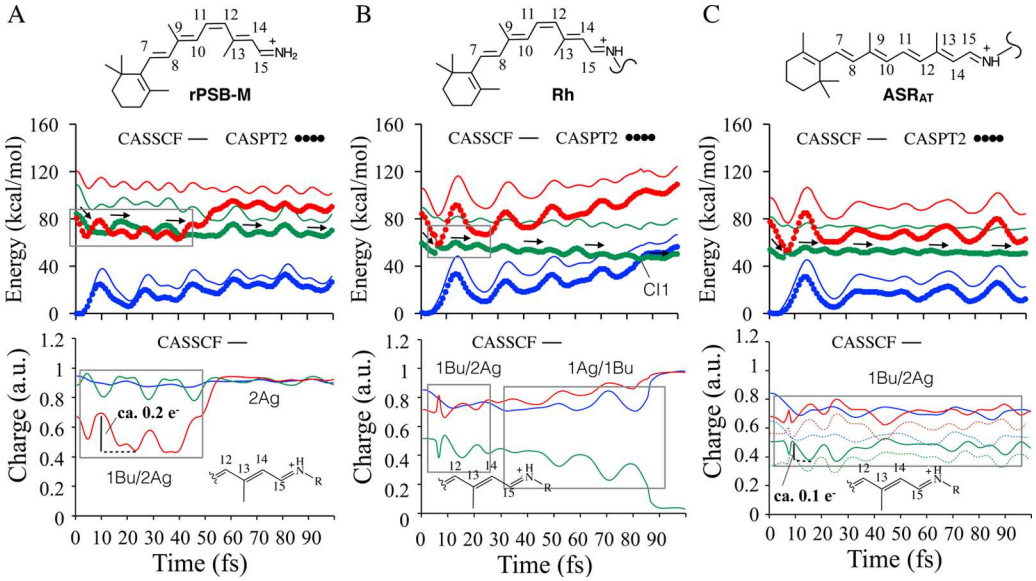

Figure 1. Environment effect on the S_1 relaxation (see stream of arrows) of rPSB. (A) CASSCF and CASPT2 energy profiles (top panels) and evolution of charge on the Schiff base side (bottom panel) of the 12-s-*trans* conformer of rPSB11 in methanol (rPSB-M) along 3-root-state-average FC trajectory. (B) Same data for rPSB11 in Rh. (C) Same data for rPSBAT in ASR_{AT}. Consistently with Scheme 1, the S_0, S_1 and S_2 PESs are represented by blue, green, and red colors, respectively. The profiles shown in bottom panels are the total positive charge on the displayed moiety (a small charge indicates 1Bu character). Dashed lines in the bottom panel of part C represent the charge on the shorter C13(Me)−C14H−C15H-NHR moiety (i.e., relevant to the C13═C14 isomerization of rPSBAT).

According to Scheme 1B, the relaxation out of the FC point may lead to a highly twisted CI1 structure or to a substantially planar CI3. Through CI3, which is energetically not far from the FC point, the chromophore may access the S_2 PES. Notice that an "attempt" to populate the S_2 PES from the S_1 PES occurs immediately after relaxation from the FC point where one has a sudden decrease (increase) of the S_2-S_1 (S_1-S_0) energy gap (see framed region). As we illustrate in Scheme 1D, a reduction of the S_2-S_1 gap may be caused by an environment preferentially stabilizing the 1Ag and 2Ag character (e.g., placing a negative charge close to the Schiff base group). CI2 is instead located much higher in energy and has the same quasi-tetra-radical electronic structure[22] documented for polyenes. In conclusion, the PSB5 calculations indicate that CI2 is hardly accessible, which means that, after population of the S_2 PES, rPSB remains unreactive until it is transferred back to S_1. Notice that the electronic states driving the photoisomerization of a model rPSB had already been described by Josef Michl and Vlasta Bonačić Koutecky in the late 1980s.[23,24] Michl and co-workers also originally highlighted the pivotal role of CIs in organic photochemical reactions and tested these hypotheses computationally.[24,25]

Below we compare three QM/MM models where rPSB is embedded in different environments. In all models, the S_0, S_1, and S_2 PES are initially (i.e., at the FC point) associated with dominating 1Ag, 1Bu and 2Ag characters, respectively. However, as document below, relaxation along the S_1 PES may lead to character variations (e.g., at a crossing or avoided crossing) increasing the unreactive 2Ag character and leading to a longer S_1 lifetime.

The Relaxation of the 11-cis rPSB in Methanol Leads to Strong 2Ag/1Bu Character Mixing. As apparent from inspection of Figure 1A, the FC trajectory of the 12-s-*trans* conformer of rPSB11 in methanol (rPSB-M) does not undergo fast decay from S_1 to S_0, at variance with the mechanism proposed in ref 12. In fact, multiple real CASPT2 crossings (or avoided crossings in the XMCQDPT2 description; see Figure S4) between the S_1 and S_2 PESs point to mixed 1Bu and 2Ag characters. This is consistent with the coupled out-of-phase oscillatory charge distributions occurring along the S_1 and S_2 PESs (see the framed region in the bottom panel in Figure 1A). More specifically, the large periodic 0.2 e^- charge variation indicates a periodic increase in the unreactive 2Ag character and explains why the photoisomerization in methanol is slow. In other words, the initial S_1 motion leads toward CI3 (i.e., a conical intersection between the 1Bu and 2Ag states) and remains in its vicinity.

Here we should also point out that, consistently with Scheme 1C, in a polar solvent the 1Ag/1Bu mixing seen along the gas-phase S_0 and S_1 PESs is lost and replaced by the 2Ag/1Bu mixing along the S_2 and S_1 PESs. This is due to the fact that, as also illustrated in Scheme 1D, polar solvents stabilize PESs featuring 1Ag and 2Ag characters (see Scheme 1D) relative to that with 1Bu character via a virtual counterion. This counterion effect is documented in Figure S5 for PSB5 interacting with a Cl^- counterion.

The analysis of the geometrical progression along the rPSB-M trajectory shows that the computed ∼20 fs period oscillations are driven by changes in the bond length alteration (BLA) coordinate defined as the difference between the average single-bond length and the average double-bond length of the rPSB backbone (see Figure S6). During the oscillations, BLA remains at slightly positive values consistently with an undeveloped double/single-bond inversion and charge transfer.

Figure 1A shows that the S_1 and S_2 crossings last for 40 fs. Then they disappear together with the 1Bu character. In order to find out why, we computed the FC trajectories at the 4- and 5-root-state-average levels. It is shown (see Figure S7) that along these trajectories, the S_3 and S_4 PES display 1Bu character, get stabilized, cross the S_2 PES, and get close to the S_1 PES for times beyond 40 fs. In other words, S_3 and S_4

DOI: 10.1021/acs.jpclett.7b02344
J. Phys. Chem. Lett. 2017, 8, 5222−5227

reinstate a partial 1Bu character beyond 40 fs, even if the S_1 PES remains dominated by the 2Ag unreactive character.

At this point, we have to stress that the reference 3-root-state-average level used in the present study is chosen as the best compromise between accuracy and information. In other words, we decided to limit the number of interacting roots to the one strictly necessary to correctly describe states that are strongly interacting with the spectroscopic/reactive state. The consequence of including additional roots and the generated artifacts are discussed in the Supporting Information (see section S6).

rPSB11 Relaxation in Rh Avoids Strong 1Bu/2Ag Character Mixing. As shown in Figure 1B, the FC trajectory for rPSB11 in Rh reaches CI1 and decay within 100 fs consistently with previous theoretical studies and spectroscopic observations (notice that, the S_1 energy profiles appear just a little flatter than the previously reported ones based on 2-root-state-average trajectories[18]). Both the CASPT2 and XMCQDPT2 energy profiles (see Figure 1B and Figure S4, respectively) display an initial 10 fs relaxation leading close to CI3 (i.e., the S_2 and S_1 PES become nearly degenerate). However, this CI3 region is immediately abandoned, allowing S_1 progression along a C11═C12 twisting coordinate. As expected, the charge distribution analysis reveals a short 1Bu/2Ag mixing along the S_1 PES (first framed region in the bottom panel of Figure 1B), which is followed by progression along a region dominated by 1Bu character and finally a terminal region (second framed region in the bottom panel of Figure 1B) experiences 1Bu/1Ag character mixing (i.e., in the CI1 region) where the S_1 and S_0 PES are almost degenerate. Notice that essentially the same behavior has been reported along a 2-root-state-average trajectory,[18] indicating that such level is adequate for Rh in line with the documented weaker interaction between S_2 and S_1 PESs.

Does the Environment Control the Photoisomerization Speed via Character Mixing? Comparison of the rPSB-M (Figure 1A) and Rh (Figure 1B) trajectories shows that, in models with the same rPSB11 chromophore and state-average level, the 2Ag/1Bu mixing is stronger in solution. This suggests that the protein environment reduces the state mixing to preserve a 1Bu character and enhance progression toward CI1 (i.e., as reported in a different context,[26] the protein environment is closer to gas-phase rather than solution). In contrast, when stronger mixing occurs, the reaction coordinate goes through a S_1 PES featuring a flat, bumpy and, ultimately, unreactive region until an event (e.g., a large twisting) occurs reinstating the 1Bu character. This mechanism explains why the photoisomerization of Rh is ultrafast but takes several picoseconds in rPSB-M.

At this point, it is important to look at rhodopsins with an isomerization time scale slower than Rh but faster than rPSB-M. ASR_{AT} is a microbial rhodopsin featuring an rPSBAT chromophore that abandons the S_1 PES on a 500−700 fs time scale.[7] The energy profiles and charge transfer evolution of the corresponding FC trajectory are reported in Figure 1C. Comparison of Figure 1A, 1B, and 1C shows that ASR_{AT} undergoes state mixing but, at a lesser extent when compared to rPSB-M. This is evident when looking at the framed region in the charge evolution diagram (bottom panel of Figure 1C) showing that the S_1 and S_2 charges are coupled. However, the magnitude of the 1Bu and 2Ag character oscillations is roughly half (ca. 0.1 e^-) of that documented for rPSB-M (ca. 0.2 e^-). Therefore, one could rank Rh, ASR_{AT} and rPSB-M as low, moderate, and high in terms of state mixing. This trend is qualitatively consistent with the isomerization time scale of each system.

The ASR_{AT} slower S_1 reactivity could be in part due to the differences its rPSBAT chromophore and the rPSB11 of Rh. This possibility has been previously discussed on the bases of 2-root-state-average FC trajectories.[18] In fact, rPSB11 differs from rPSBAT in a number of ways: (i) it features an effectively shorter conjugated chain due to out-of-plane twisting of the β-ionone ring, (ii) the ca. 10 degrees pretwist about the C11═C12 double bond increases the splitting between the S_1 and S_2 energies, (iii) the reaction coordinate dominated by the twisting about C11═C12 double bond rather than C13═C14 double bond (as in microbial rhodopsins) separates the S_1 and S_2 more effectively and, (iv) the 11-*cis* configuration of the C10−C11═C12−C13 moiety introduces a strain increasing the PES slope along the coordinate leading to CI1. Therefore, we attribute the difference in S_1 lifetime of Rh and ASR_{AT} to both environmental effects decreasing the state mixing and the type of rPSB isomer bound to the protein. A previous study employing a simplified gas-phase chromophore model with a counterion has discussed the possible involvement of S_1/S_2 crossings in controlling the rPSB photoreactivity.[27] In this work, the authors have attributed slow photoisomerization to S_1/S_2 crossing and recrossing processes creating shallow barriers, however, the dynamics and nature of the state mixing have not been considered. A recent computational study reported that 10-methyl-rPSBAT (i.e., rPSBAT with a methyl substituent at C10) shows, surprisingly, a femtosecond decay time in solution, which was attributed to an increased energy gap between S_2 and S_1.[28] We tested this substituent effect in the protein environment by propagating a 3-root-state-average FC trajectory for ASR_{AT} hosting 10-methyl-rPSBAT (10Me-ASR_{AT}). Although, as we showed above, the ASR_{AT} has a slow reactivity, 10Me-ASR_{AT} reaches the CI within 110 fs, consistently with a decrease in 1Bu/2Ag coupling (see Figure S12) and the results in ref 28.

Electronic Character Mixing and Rhodopsin Evolution. Above we have used an approximate tool, namely, three short FC trajectories, to support a correlation between S_1 lifetime and 1Bu/2Ag character mixing. If one hypothesizes that ultrafast isomerization provides an adaptive advantage (i.e., for instance a higher light sensitivity), the results above imply that the protein sequence will evolve to *minimize* 2Ag/1Bu mixing along the S_1 PES. In this sense, visual pigments like Rh would be considered better adapted than the ASR_{AT} light sensor. The results above can also be interpreted in terms of the validity of a 2-state (S_1 and S_0) isomerization model for fast reacting rhodopsins (e.g., Rh) and a 3-state (S_2, S_1, and S_0) model for slower reacting rhodopsins (e.g., ASR_{AT}) and the solution environment. A 3-state model has been previously proposed for microbial bacteriorhodopsins (bR), which displays slow and complex excited state dynamics.[15]

The conclusions above depend on the validity of the adopted 3-root-state-average trajectories. In fact, the geometrical progression is determined by the 3-root-state-average CASSCF/AMBER PES. The assumption of a qualitative equivalence between these PES and those computed, for instance, at the more accurate XMCQDPT2/AMBER or equivalently XMS-CASPT2/AMBER levels, needs to be carefully investigated in the near future (for instance, by exploiting the recently reported XMS-CASPT2 analytical gradients).[29] Recently S_2/S_1 crossings have been documented for another microbial rhodopsin: channelrhodopsin.[30] Con-

DOI: 10.1021/acs.jpclett.7b02344
J. Phys. Chem. Lett. 2017, 8, 5222−5227

sistently with our conclusion, the measured shortest excited state lifetime is 450 fs and therefore several times longer than that for Rh.[31]

■ ASSOCIATED CONTENT

Supporting Information

The Supporting Information is available free of charge on the ACS Publications website at DOI: 10.1021/acs.jpclett.7b02344.

Computational details for methodology, optimized CIs of model chromophores, effect of XMCQDPT2 level of theory, effect of counterion on electronic state coupling, BLA, energy and charge profiles along rPSB-M trajectories, investigation of the origin of artifactual state mixing, and effect of 10-Methyl substitution on ASR trajectory (PDF)

■ AUTHOR INFORMATION

Corresponding Author

*E-mail: molivuc@bgsu.edu.

ORCID

Massimo Olivucci: 0000-0002-8247-209X

Notes

The authors declare no competing financial interest.

■ ACKNOWLEDGMENTS

This work was supported in part by the Italian MIUR for funding (PRIN 2015) and, in part, by the National Science Foundation under Grant No. CHE-1710191. M.O. is grateful to the Ohio Supercomputer Center for granted computer time. M.O. and Y.O. are grateful to the University of Strasbourg for a USIAS 2015 fellowship.

■ REFERENCES

(1) Spudich, J. L.; Yang, C. S.; Jung, K. H.; Spudich, E. N. Retinylidene Proteins: Structures and Functions from Archea to Humans. *Annu. Rev. Cell Dev. Biol.* **2000**, *16*, 365−392.

(2) Kandori, H.; Shichida, Y.; Yoshizawa, T. Photoisomerization in Rhodopsin. *Biochemistry* **2001**, *66*, 1197−1209.

(3) Ernst, O. P.; Lodowski, D. T.; Elstner, M.; Hegemann, P.; Brown, L. S.; Kandori, H. Microbial and Animal Rhodopsins: Structures, Functions, and Molecular Mechanisms. *Chem. Rev.* **2014**, *114*, 126−163.

(4) Kukura, P.; McCamant, D. W.; Yoon, S.; Wandschneider, D. B.; Mathies, R. A. Structural Observation of the Primary Isomerization in Vision with Femtosecond-Stimulated Raman. *Science* **2005**, *310*, 1006−1009.

(5) Schoenlein, R.; Peteanu, L.; Mathies, R.; Shank, C. The First Step in Vision: Femtosecond Isomerization of Rhodopsin. *Science* **1991**, *254*, 412−415.

(6) Peteanu, L. A.; Schoenlein, R. W.; Wang, Q.; Mathies, R. A.; Shank, C. V. The First Step in Vision Occurs in Femtoseconds: Complete Blue and Red Spectral Studies. *Proc. Natl. Acad. Sci. U. S. A.* **1993**, *90*, 11762−11766.

(7) Cheminal, A.; Leonard, J.; Kim, S.-Y.; Jung, K.-H.; Kandori, H.; Haacke, S. 100 fs Photoisomerization with Vibrational Coherences but Low Quantum Yield in Anabaena Sensory Rhodopsin. *Phys. Chem. Chem. Phys.* **2015**, *17*, 25429−25439.

(8) Cheminal, A.; Léonard, J.; Kim, S.-Y.; Jung, K.-H.; Kandori, H.; Haacke, S. Steady State Emission of the Fluorescent Intermediate of Anabaena Sensory Rhodopsin as a Function of Light Adaptation Conditions. *Chem. Phys. Lett.* **2013**, *587*, 75−80.

(9) Wand, A.; Friedman, N.; Sheves, M.; Ruhman, S. Ultrafast Photochemistry of Light-Adapted and Dark-Adapted Bacteriorhodopsin: Effects of the Initial Retinal Configuration. *J. Phys. Chem. B* **2012**, *116*, 10444−10452.

(10) Becker, R. S.; Freedman, K.; Hutchinson, J. A.; Noe, L. J. Kinetic Study of the Photoisomerization of a Protonated Schiff Base of 11-cis-Retinal Over the Picosecond-to-Second Time Regimes. *J. Am. Chem. Soc.* **1985**, *107*, 3942−3944.

(11) Kandori, H.; Katsuta, Y.; Ito, M.; Sasabe, H. Femtosecond Fluorescence Study of the Rhodopsin Chromophore in Solution. *J. Am. Chem. Soc.* **1995**, *117*, 2669−2670.

(12) Bassolino, G.; Sovdat, T.; Soares Duarte, A.; Lim, J. M.; Schnedermann, C.; Liebel, M.; Odell, B.; Claridge, T. D. W.; Fletcher, S. P.; Kukura, P. Barrierless Photoisomerization of 11-cis Retinal Protonated Schiff Base in Solution. *J. Am. Chem. Soc.* **2015**, *137*, 12434−12437.

(13) Huppert, D.; Rentzepis, P. M. Time-Resolved Luminescence Study of Protonated Schiff Bases. *J. Phys. Chem.* **1986**, *90*, 2813−2816.

(14) Logunov, S. L.; Song, L.; El-Sayed, M. Excited-State Dynamics of a Protonated Retinal Schiff Base in Solution. *J. Phys. Chem.* **1996**, *100*, 18586−18591.

(15) Gai, F.; Hasson, K. C.; McDonald, J. C.; Anfinrud, P. A. Chemical Dynamics in Proteins: the Photoisomerization of Retinal in Bacteriorhodopsin. *Science* **1998**, *279*, 1886−1891.

(16) Gozem, S.; Melaccio, F.; Luk, H. L.; Rinaldi, S.; Olivucci, M. Learning from Photobiology How to Design Molecular Devices Using a Computer. *Chem. Soc. Rev.* **2014**, *43*, 4019−4036.

(17) Sinicropi, A.; Martin, E.; Ryazantsev, M.; Helbing, J.; Briand, J.; Sharma, D.; Leonard, J.; Haacke, S.; Cannizzo, A.; Chergui, M.; et al. An Artificial Molecular Switch That Mimics the Visual Pigment and Completes its Photocycle in Picoseconds. *Proc. Natl. Acad. Sci. U. S. A.* **2008**, *105*, 17642−17647.

(18) Luk, H. L.; Melaccio, F.; Rinaldi, S.; Gozem, S.; Olivucci, M. Molecular Bases for the Selection of the Chromophore of Animal Rhodopsins. *Proc. Natl. Acad. Sci. U. S. A.* **2015**, *112*, 15297−15302.

(19) Frutos, L. M.; Andruniów, T.; Santoro, F.; Ferré, N.; Olivucci, M. Tracking the Excited-State Time Evolution of the Visual Pigment with Multiconfigurational Quantum Chemistry. *Proc. Natl. Acad. Sci. U. S. A.* **2007**, *104*, 7764−7769.

(20) Andersson, K.; Malmqvist, P.-Å.; Roos, B. O. Second-Order Perturbation Theory with a Complete Active Space Self-Consistent Field Reference Function. *J. Chem. Phys.* **1992**, *96*, 1218−1226.

(21) Granovsky, A. A. Extended Multi-Configuration Quasi-Degenerate Perturbation Theory: The New Approach to Multi-State Multi-Reference Perturbation Theory. *J. Chem. Phys.* **2011**, *134*, 214113.

(22) Celani, P.; Garavelli, M.; Ottani, S.; Bernardi, F.; Robb, M. A.; Olivucci, M. Molecular Trigger for Radiationless Deactivation of Photoexcited Conjugated Hydrocarbons. *J. Am. Chem. Soc.* **1995**, *117*, 11584−11585.

(23) Bonačić-Koutecký, V.; Schöffel, K.; Michl, J. Critically Heterosymmetric Biradicaloid Geometries of Protonated Schiff Bases. *Theor. Chim. Acta* **1987**, *72*, 459−474.

(24) Michl, J.; Bonačić-Koutecký, V. *Electronic aspects of organic photochemistry*; Wiley-Interscience: NewYork, 1990.

(25) Schapiro, I.; Ryazantsev, M. N.; Frutos, L. M.; Ferré, N.; Lindh, R.; Olivucci, M. The Ultrafast Photoisomerizations of Rhodopsin and Bathorhodopsin Are Modulated by Bond Length Alternation and HOOP Driven Electronic Effects. *J. Am. Chem. Soc.* **2011**, *133*, 3354−3364.

(26) Coto, P. B.; Strambi, A.; Ferré, N.; Olivucci, M. The Color of Rhodopsins at the Ab Initio Multiconfigurational Perturbation Theory Resolution. *Proc. Natl. Acad. Sci. U. S. A.* **2006**, *103*, 17154−17159.

(27) Cembran, A.; Bernardi, F.; Olivucci, M.; Garavelli, M. The Retinal Chromophore/Chloride Ion Pair: Structure of the Photoisomerization Path and Interplay of Charge Transfer and Covalent States. *Proc. Natl. Acad. Sci. U. S. A.* **2005**, *102*, 6255−6260.

(28) Demoulin, B.; Altavilla, S. F.; Rivalta, I.; Garavelli, M. Fine Tuning of Retinal Photoinduced Decay in Solution. *J. Phys. Chem. Lett.* **2017**, *8*, 4407−4412.

DOI: 10.1021/acs.jpclett.7b02344
J. Phys. Chem. Lett. 2017, 8, 5222−5227

(29) Shiozaki, T.; Győrffy, W.; Celani, P.; Werner, H.-J. Communication: Extended Multi-State Complete Active Space Second-Order Perturbation Theory: Energy and Nuclear Gradients. *J. Chem. Phys.* **2011**, *135*, 081106.
(30) Dokukina, I.; Weingart, O. Spectral Properties and Isomerisation Path of Retinal in C1C2 Channelrhodopsin. *Phys. Chem. Chem. Phys.* **2015**, *17*, 25142−25150.
(31) Hontani, Y.; Marazzi, M.; Stehfest, K.; Mathes, T.; van Stokkum, I. H. M.; Elstner, M.; Hegemann, P.; Kennis, J. T. M. Reaction Dynamics of the Chimeric Channelrhodopsin C1C2. *Sci. Rep.* **2017**, *7*, 7217.

DOI: 10.1021/acs.jpclett.7b02344
J. Phys. Chem. Lett. 2017, 8, 5222−5227